

Wiley Analytical Science Virtual Conference

November 9-17



For the 3rd time, The Wiley Analytical Science Conference is back!

It's all happening November 9 - 17

The Wiley Analytical Science Virtual Conference will bring together thousands of researchers and practitioners to share current developments in science and industry. Join for exciting presentations from experts in the fields of analytical and bioanalytical chemistry, pharmaceutical research, materials science, lab automation, and related disciplines.

Register to learn about recent developments & applications in:

- Microscopy
- Spectroscopy
- Mass Spectrometry
- Separation Science
- Much more!

Register here

3D Bioprinting of Cell-Laden Hydrogels for Improved Biological Functionality

Sarah M. Hull, Lucia G. Brunel, and Sarah C. Heilshorn*

The encapsulation of cells within gel-phase materials to form bioinks offers distinct advantages for next-generation 3D bioprinting. 3D bioprinting has emerged as a promising tool for patterning cells, but the technology remains limited in its ability to produce biofunctional, tissue-like constructs due to a dearth of materials suitable for bioinks. While early demonstrations commonly used viscous polymers optimized for printability, these materials often lacked cell compatibility and biological functionality. In response, advanced materials that exist in the gel phase during the entire printing process are being developed, since hydrogels are uniquely positioned to both protect cells during extrusion and provide biological signals to embedded cells as the construct matures during culture. Here, an overview of the design considerations for gel-phase materials as bioinks is presented, with a focus on their mechanical, biochemical, and dynamic gel properties. Current challenges and opportunities that arise due to the fact that bioprinted constructs are active, living hydrogels composed of both acellular and cellular components are also evaluated. Engineering hydrogels with consideration of cells as an intrinsic component of the printed bioink will enable control over the evolution of the living construct after printing to achieve greater biofunctionality.

in 3D bioprinting, as they can provide mechanical protection and structural support during the printing process, be tuned to recapitulate many features of the native ECM, and be customized to influence cell–gel interactions postprinting. While several excellent reviews have recently been written within the broad topic of materials design for bioprinting,^[1–4] here, we will focus on the design and development of hydrogel bioinks that exist in the gel phase during the entire printing process and include embedded cells as a strategy for improving the achievable biofunctionality of 3D bioprinted constructs.

3D bioprinting has grown out of the field of 3D printing. Although the process of 3D printing using thermoplastics has advanced greatly with capabilities to create very complex structures, these constructs are often neither biologically compatible nor mimetic of native tissue. Physiologic cell volume fractions, which range *in vivo* from 1% to 2% in cartilage^[5,6] up to \approx 80%

in liver^[7–10] and 90% in muscle,^[10–13] are difficult to achieve by seeding cells on top of 3D printed thermoplastic scaffolds, so biomimetic constructs often utilize hydrogels to encapsulate larger volume fractions of cells. Here, we define a bioink for 3D bioprinting to be a composite mixture of polymeric material and living cells that is deposited and solidified into a prespecified geometry.^[14] We define hydrogels as water-swollen, insoluble polymer networks formed through chemical or physical crosslinking. Several 3D printing techniques have been translated for the bioprinting process—including inkjet, extrusion, laser-assisted, and stereolithography printing^[15]—but we will focus on microextrusion bioprinting techniques, since these are most commonly used with hydrogel materials. Microextrusion processes use continuous pneumatic pressure or mechanical forces that are motor or screw-driven to dispense the bioink from the print nozzle as an uninterrupted filament.^[16] As compared to 3D printing of thermoplastics, the presence of living cells in bioprinting greatly limits printing variables such as temperature, pH, and pressure as well as the material properties of the bioink.

Due to a scarcity of suitable materials to comprise bioinks, the field of 3D bioprinting has suffered from challenges in fabricating constructs that replicate both the structural complexity and biological functionality of native tissues. Most tissues *in vivo* have stiffness ranging from 0.1 to 100 kPa, so materials that match physiological mechanical properties must

1. Introduction

The technique of 3D bioprinting has demonstrated potential for the fabrication of complex constructs that bear resemblance in form and functionality to native tissues. Native tissues are living composites of cells embedded within a complex extracellular matrix (ECM) of biopolymers that provide structural support and biochemical cues to the cells. By recapitulating the micro-environmental features of tissues, bioprinted constructs with precisely patterned cells and polymeric components can serve as *in vitro* models of native tissue for basic research or can be translated into the clinic as implantable constructs. As a class of materials, hydrogels are uniquely suited for such applications

S. M. Hull, L. G. Brunel
Department of Chemical Engineering
Stanford University
Stanford, CA 94305, USA

S. C. Heilshorn
Department of Materials Science and Engineering
Stanford University
Stanford, CA 94305, USA
E-mail: heilshorn@stanford.edu

 The ORCID identification number(s) for the author(s) of this article can be found under <https://doi.org/10.1002/adma.202103691>.

DOI: 10.1002/adma.202103691

be similarly soft.^[17,18] Since soft constructs are often not self-supporting, it is difficult to bioprint soft materials into complex 3D geometries. In addition, a number of biological challenges exist in bioprinting, including low cell viability, poor homogeneity within the construct, and the inability to sufficiently guide cell phenotype. Early demonstrations of bioprinting commonly used inks of viscous, solution-phase polymers (i.e., not hydrogels) optimized for printability in air that were then crosslinked into hydrogels postprinting (e.g., through use of light-initiated chemical reactions).^[19] These materials often lacked biological functionality, had cell viability challenges, and prevented the fabrication of complex structures. While many advances have been made since these early pioneering demonstrations, a remaining challenge for the field is the ability of bioink materials to support cells through all stages of printing: 1) while suspended in the syringe, 2) during extrusion through the nozzle, 3) during any material crosslinking steps, and 4) as the final construct matures to become more tissue-like after printing.^[20] Fortunately, decades of polymer science and tissue engineering research have provided detailed insights into cell–hydrogel interactions. Future success in the bioprinting field will be dependent on applying these insights to achieve printed constructs with high levels of both geometric complexity and biological functionality.

The combination of cells with advanced hydrogels to form bioinks that exist in the gel phase during all stages of the bioprinting process leverages the unique properties of hydrogels to expand the range of achievable physical structures and biological properties. Our review begins with a focus on the enabling mechanical and biochemical properties of hydrogels that make their use as bioink materials in 3D bioprinting beneficial. In this section, design strategies and case-studies of bioinks that exist in the gel phase both pre- and post-printing are discussed. More recently, as the 3D bioprinting community strives to fabricate more biologically functional tissue mimics, a growing appreciation for the fact that all bioinks are dynamic, living materials has begun to emerge. Indeed, most tissues in our body are active hydrogels composed of nonliving polymers and living cells. Thus, in our forward-looking perspective section of this review, we highlight opportunities to leverage cell–hydrogel interactions that occur postprinting to evolve biologically functional tissue.

2. Bioink Gels

Hydrogels are attractive materials to combine with cells for use as bioinks in 3D bioprinting since they can mechanically and biochemically support cells during and after the printing process. Hydrogels are water swollen networks of polymers that can provide a cell-instructive, aqueous environment for 3D cell culture. The network is held together by physical interactions and/or covalent bonds called crosslinks. When there are very few or no crosslinks, these materials can have fluid-like properties, and when more crosslinks are present, these materials typically have more solid-like characteristics. As gel-phase materials, hydrogels are well suited to be used as inks for 3D bioprinting. Here, we focus on bioinks that are in the gel-phase both in the syringe and after printing. We highlight the

advantages of gel-phase bioinks in each stage of the printing process and then explore the material requirements that enable them to be used as bioinks (Figure 1).

2.1. Advantages of Gel-Phase Bioinks

2.1.1. In the Print Cartridge

In the print cartridge, hydrogels can maintain a homogenous cell suspension by preventing cell sedimentation. In a viscous fluid, gravity (F_g) pulls cells toward the bottom of the print cartridge, which can lead to cell sedimentation and uneven cell distribution within the ink prior to extrusion.^[20] This excess gravitational force is opposed by Stokes' drag (F_d), and by requiring the force balance $F_g = F_d$, the settling velocity can be solved for as

$$v = \frac{2(\rho_c - \rho_f)}{9\mu} g R^2 \quad (1)$$

where g is the gravitational field strength, R is the radius of the cell, ρ_c is the mass density of the cell, ρ_f is the mass density of the fluid, and μ is the dynamic viscosity. As cells sediment, they are no longer homogeneously dispersed in the ink. This can lead both to clogged nozzles and to an uneven distribution of cells in the final printed structure (i.e., the first printed layers would contain more cells than subsequent layers). These problems associated with cell sedimentation are amplified when creating larger and more complex constructs since these structures will typically require longer print times. Printing full-scale tissues or organs may take hours up to days.^[21] Gel-phase bioinks can be used to overcome the challenges presented by cell sedimentation. This can be achieved either by blending in viscosity modifiers to slow down sedimentation or by incorporating weak crosslinking into the bioink design to increase the yield stress.^[20] Such hydrogels would prevent cell sedimentation, but also remain printable as they can flow once a force is applied.

2.1.2. During Printing

While printing, a hydrogel can protect cells from shear stresses and subsequent cell membrane damage, which can improve cell viability in the printed construct. Cells experience mechanical stresses during extrusion that can rupture their membranes and reduce cell viability.^[22] When cells are extruded through a needle within a low viscosity fluid, demonstrations have shown that up to 40% of the cells do not survive the process, likely due to membrane damage caused by extensional flow within the needle.^[23] In addition to directly damaging the cell membrane, shear stresses have also been shown to affect cell morphology, cytoskeletal organization, and gene and protein expression, though the effects of these changes on the biological functionality of 3D printed structures has yet to be investigated.^[1,24–26] Many gel-phase bioinks can protect cells from these shear forces if the material undergoes plug flow at the center of its flow profile.^[27] For this to occur, the portion of the gel adjacent

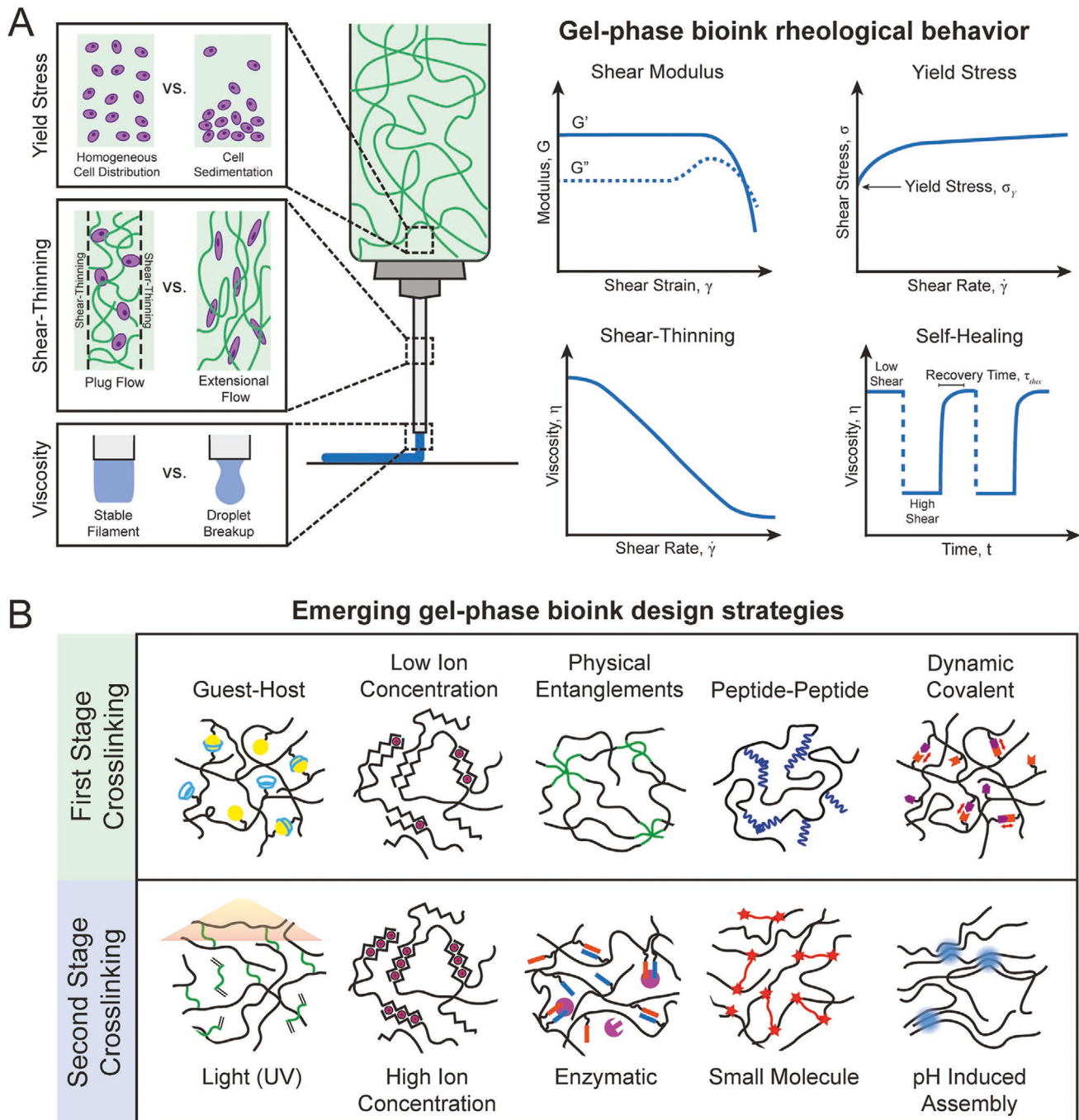


Figure 1. Design considerations for hydrogel-based bioinks and dual-stage crosslinking strategies for advanced bioinks. A) Hydrogel-based bioinks are ideally yield-stress fluids with shear-thinning properties and high enough viscosities to allow for stable filament extrusion. The presence of a yield stress means that prior to printing, the bioink material is solid-like, which aids in preventing cell sedimentation in the extruder, but after sufficient force is applied, the ink can yield and flow. Shear-thinning of the bioink at the extruder wall can allow the center of the gel to pass through the extruder as a relatively undeformed plug, protecting cells from membrane-damaging mechanical forces. B) Potential first- and second-stage crosslinking strategies for dual-stage inks that are gels both before and after printing. The mode of first-stage crosslinking defines the material's rheological behavior during printing. Second-stage crosslinking refers to an optional postprint "curing" step, which produces a construct with greater structural integrity and with the desired mechanical properties.

to the syringe wall is shear-thinned and can then act as a lubricating layer, allowing the rest of the gel to pass through the extruder as a relatively undeformed plug. Thus, cells in the plug

flow region are not exposed to membrane-damaging mechanical forces and remain viable during the extrusion process. In contrast, in sol-phase inks cells typically experience extensional

flow rather than plug flow, and the increased viscosity needed to print sol-phase inks can actually lead to even greater shear stress imparted on the cell membrane.^[28] Therefore, a key advantage of using hydrogels in bioinks is their ability to shield cells from mechanical stresses during extrusion, preventing cell death and any unintended cell phenotype changes.

2.1.3. Postprinting

After printing, hydrogels can provide a 3D culture environment that supports cellular survival and function. Hydrogels are widely used for 3D cell culture because they provide a cell-compatible, aqueous environment that can emulate many of the biochemical and mechanical features of native tissue.^[29] Their high water content and permeability allow for facile diffusion of nutrients and waste to and from encapsulated cells. In addition, they can provide numerous signals to instruct cell phenotype, differentiation, growth, and migration.^[30] Historically, hydrogels have been used extensively for tissue engineering applications, and the decades of previous research on hydrogels can be leveraged into bioink designs.^[31–33] Based on this knowledge, hydrogels can be engineered to meet both the structural and biological demands of increasingly complex, tissue-like scaffolds that mimic *in vivo* architectures.

2.2. Material Requirements for Gel-Phase Bioinks

2.2.1. Rheological Properties

To be translated into bioinks, hydrogels must be made printable while also retaining their cell compatibility, which remains a key challenge that has limited the progression of 3D printing technologies. The rheological properties of the bioink play a large role in its ability to be extruded and to protect cells during the printing process. Nevertheless, reported rheological measurements are still not consistent across the bioprinting field and there is no clear consensus on what it means for a material to be “printable.” Generally, for extrusion-based bioprinting, printability refers to the ability of the material to be extruded through a syringe, to form consistent filaments during deposition, and to maintain shape fidelity following printing such that the final structure resembles the intended design as closely as possible.^[3] Several methodologies, both quantitative and qualitative, have been suggested to assess printability, and have been summarized in other recent reviews.^[34–36] However, it remains challenging to compare different bioink materials, especially since common metrics such as print resolution and shape fidelity have been shown to be highly dependent on printing conditions such as flow rate, pressure, nozzle size, path design, temperature, and more.^[28,37] Thus, it is clear that more standardized, quantitative metrics would be useful for evaluating new bioink designs. Here, we focus our discussion on the rheological requirements that contribute to bioink extrudability and long-term stability as well as how these material properties affect cellular behavior within the printed scaffold.

Shear Modulus: Hydrogels can exhibit both viscous and elastic behaviors in a time-dependent manner. The contribution

of each of these components can be determined by measuring the shear storage modulus, G' , and the shear loss modulus, G'' , typically against time, frequency, or strain. G' represents the elastic component (also referred to as the stiffness of the material) and G'' represents the viscous component (the liquid-like response of the material). When $G' > G''$, the material behaves more like an elastic solid and is considered to be in the gel phase; in contrast, when $G' < G''$, the material behaves more like a viscous liquid and is thus in the sol phase (Table 1). Depending on the molecular weight and geometric structure of the polymers composing a hydrogel, the resulting rheological properties can range from being largely elastic (i.e., without significant time-dependence) to viscoelastic (i.e., with large time-dependence).^[45] As previously discussed, gel-phase bioinks offer several advantages over sol-phase inks, most notably in that they better preserve cell viability throughout the printing process.

Yield Stress: The yield stress represents the stress required for a gel to begin to flow. The presence of a yield stress implies that prior to printing (that is, prior to any stress being applied), the material is solid-like, which aids in preventing cell sedimentation in the extruder. For microextrusion printing techniques, sufficient pressure must then be applied (either pneumatic-, piston-, or screw-driven) such that the gel can yield and flow. Recent studies suggest that high yield stresses that result in sharp decreases in viscosity lead to gels that are more readily printable, as measured by consistent filament formation.^[39] However, if the yield point is too high, then very large pressures may be needed that are not achievable using currently available extruders and could also lead to significant cell death.^[46]

Viscosity: The viscosity of a bioink is a measure of its resistance to flow. For extrusion-based 3D bioprinting, viscosity influences the ability of the ink to be extruded and plays a role in print fidelity. In general, increasing the viscosity of the bioink improves printability since higher viscosity inks impede droplet formation, so the ink can instead be printed as a continuous filament.^[47] If the material is printed in a layer-by-layer fashion, high viscosity inks can also increase print resolution and shape retention after printing as the structure is able to support itself. However, inks that are too viscous can also clog the print needle since they are more resistant to flow, leading to inconsistent deposition. In addition, highly viscous solutions can increase the shear damage imparted on the cell membrane, which could decrease cell viability.^[48] Therefore, the viscosity of the ink must be tuned to strike a balance between improved printability and maintaining cell viability. The viscosity is influenced by parameters such as polymer molecular weight, polymer concentration, degree of crosslinking, and temperature;^[49] thus, there exists a large phase space with which to optimize the ink to maximize both printability and cell survival.

Table 1. Rheological properties for a selection of sol-phase versus gel-phase bioinks.

Bioink material phase	Viscosity [Pa s]	Yield stress [Pa]	Refs.
Gel-phase ($G' > G''$)	$\approx 20\text{--}6 \times 10^5$	20–2400	[38–41]
Sol-phase ($G' < G''$)	$\approx 0.1\text{--}30$	None	[42–44]

Shear-Thinning: Shear-thinning is a behavior in which the viscosity decreases as the shear rate increases. Shear-thinning behavior is observed rheologically by alternating periods of low and high strains and observing if the hydrogel decreases in viscosity under high strain and then recovers when the strain is reduced. Shear-thinning hydrogels are well suited for 3D bioprinting because they can easily flow under high shear rates present in the print nozzle, but then undergo time-dependent recovery of their initial properties, which can aid in structure stabilization. Additionally, as previously mentioned, shear-thinning at the extruder wall allows the center of the gel to pass through the extruder as a relatively undeformed plug, protecting cells from membrane-damaging mechanical forces.^[23,27] The mechanism that leads to shear-thinning behavior is specific for each polymer system, but often is the result of self-assembly due to weak, physical interactions (e.g., hydrophobic interactions, hydrogen bonding, and electrostatic attractions).^[50] Collectively, these interactions can lead to the formation of a stable network through physical or chemical crosslinks. While printing, some of these crosslinks disassemble, enabling the gel to be shear-thinned, fluid-like, and extrudable. After the material is extruded and the stress is removed, the crosslinks can reassemble to reform the network.

Self-Healing: Self-healing behavior is defined by a material's recovery after an applied shear stress is removed. This can be determined rheologically by introducing a large deformation and then monitoring the recovery of the shear modulus or viscosity over time once the stress is reduced. This is analogous to what occurs during extrusion bioprinting, in which a large force is applied to the print syringe, causing the material to decrease in viscosity and flow more like a fluid. Then, the material should ideally recover its initial viscosity after extrusion and return to a solid-like state. The time required for this transition to occur is referred to as the recovery time or the thixotropic time. Rapid self-healing behavior, that is, a short recovery time, has been shown to improve print fidelity and shape retention since the material will be self-supportive after extrusion.^[51]

Postprinting Mechanical Properties: The material properties of the bioink will also determine the ultimate mechanical properties of the printed construct. This is important not only in that the hydrogel network must be robust enough to retain its shape postprinting, but also in that the gel mechanics will affect cellular behavior. It is well-established that cells are exquisitely sensitive to the mechanical properties of their surrounding matrix.^[52] In particular, gel stiffness has been shown to regulate cell spreading, migration, proliferation, gene expression, and differentiation.^[53–56] Thus, the final stiffness of the scaffold should be optimized to elicit the chosen cell response for the intended application. In addition, on a macroscopic level, if the bioprinted construct is to be implanted into the body, it is often desirable for the stiffness to be similar to that of the native tissue so as to avoid a mechanical mismatch.^[57] Bioink stiffness can be tuned by modulating the total polymer concentration or the crosslink density.

Beyond stiffness, recent work has demonstrated that additional viscoelastic properties can also have a profound effect on cellular behavior. Physiological ECM components exhibit stress relaxation; that is, they are able to dissipate the energy of an applied stress over time. This is in contrast to purely

elastic materials, in which this energy is stored. For hydrogels containing weak crosslinks, stress relaxation can arise from crosslink unbinding and rearrangement. This behavior can be cell-induced: as cells bind to the matrix and apply force or strain, they can actively remodel the matrix. Some cell types are sensitive to changes in gel stress relaxation rates.^[58] Materials that exhibit fast stress relaxation have been shown to increase cell spreading and proliferation, and biased mesenchymal stromal cells (MSCs) toward an osteogenic lineage commitment.^[59,60] Dynamic hydrogels have been developed to allow for cellular remodeling of the network and tuning of stress relaxation rates, and there is much interest in translating such materials into bioinks.

Support Materials: In addition to the cell-laden bioink, hydrogels are also commonly used in 3D bioprinting as support materials. These support materials include so-called "sacrificial inks" and "support baths" that can temporarily provide mechanical support to the bioink during the printing process. Hydrogels with reversible sol–gel phase behavior have been used as temporary sacrificial inks to enable the printing of void spaces, including perfusable channels.^[61,62] Hydrogels with thixotropic mechanical properties can be used as support baths that enable the printing of complex structural features with increased print resolution by providing physical confinement during printing.^[63–65] The use of gel-phase support materials has greatly increased both the complexity of printed geometries and the range of materials that can be used as bioinks, as recently reviewed elsewhere.^[66,67]

2.2.2. Biochemical Properties

In addition to providing structural support, the bioink can also provide biochemical signals that instruct cell behavior. In native tissue, cells interact with the extracellular environment through cell surface receptors, including those that bind to the surrounding matrix, to soluble factors, and to neighboring cells.^[68–70] Natural biopolymers such as collagen, gelatin, hyaluronic acid, and fibrin have been used as bioinks since they already contain an array of biochemical signals, such as cell-adhesive domains, that can help maintain high cell viability and proliferation rates within printed structures.^[42,71–75] However, most naturally derived materials suffer from batch-to-batch variation; therefore, it may be challenging to produce them in a manner that ensures they are reproducibly printable. In addition, the rheological and mechanical properties of these materials are often not tunable without introducing additional functionality.

The biochemical cues presented by the ink should promote cellular function and, ideally, be tuned to fit each individual cell type. Incorporating further biochemical signals beyond those present in natural ECM components and understanding how cell–material interactions impact the biological functionality of the printed structure will be critical for engineering more complex, printed tissues. While there are many examples of incorporating biochemical cues into hydrogels in the broader biomaterials field, little has been explored in using these same cues in bioprinting. Thus, many opportunities exist for designing advanced hydrogel bioinks: motifs such as cell adhesive ligands can be added to the polymer backbone itself, proteins including

growth factors or cytokines can be tethered to the polymer network, or soluble factors can be added to the aqueous solvent of the hydrogel. We will discuss these design opportunities further in the future perspective portion of this review.

2.3. Crosslinking Approaches

For bioinks to satisfy the material requirements outlined above, they should ideally be in the gel phase both in the syringe and after printing. Here, we refer to such materials as “dual-stage crosslinked.” First-stage crosslinking defines the material’s rheological behavior during printing, while second-stage crosslinking determines the final mechanical properties. The first-stage of crosslinking is already present in the syringe: the ink acts as a weak gel below its yield point, so the cells remain suspended and viable. A weak gel can be formed through physical entanglements of the polymer itself or by incorporating either reversible bonds or a small number of covalent crosslinks. Examples of first-stage crosslinking techniques include ionic crosslinking, guest–host interactions, peptide–peptide assembly, dynamic covalent chemistries, and nonspecific physical entanglements (Figure 1). When a force is applied to the syringe, physical or dynamic crosslinks can disassemble, and the gel will yield and flow. After printing, these crosslinks can reassemble to again form a weak gel. In some cases where the material rapidly self-heals, no further crosslinking strategies have been employed; that is, the first- and second-stage crosslinking mechanism is the same. This includes materials crosslinked by guest–host interactions and dynamic covalent chemistries. However, many challenges remain in making these materials both printable and stable, as the dynamic nature of the crosslinks can lead to swelling, erosion, and creep behavior.^[76–78] For an extended discussion on dynamic hydrogels and the challenges associated with incorporating these materials into bioink designs, we point the interested reader to another recent review on the topic.^[79]

Therefore, to produce a construct with increased structural integrity or to alter the postprinting mechanical properties to be different from those in the print syringe, a second type of crosslinking can occur after extrusion. This process, also referred to as “curing,” further stabilizes the final structure and allows it to be used in downstream applications. These crosslinks are often stronger and more permanent bonds than first-stage crosslinks, as they must maintain long-term structural integrity of the printed gel. Examples include UV light-induced crosslinking, pH mediated gelation, enzymatic crosslinking, thermal gelation, and small molecule covalent crosslinkers. Due to the presence of cells in the bioink before and after extrusion, both stages of crosslinking should be as cell-friendly as possible. This limits the application of certain crosslinking strategies and chemistries in bioink design. For example, while acidified collagen has been used to successfully print complex mimics of *in vivo* structures, the low pH of the ink precludes the inclusion of cells.^[80] Only after the pH has been raised to induce gelation can cells be included; therefore, cells must either be printed separately or seeded on top of the printed collagen structure. Alternative strategies, such as using bioorthogonal crosslinkers, are being developed to

overcome these shortcomings to create inks that are more cell-friendly and can be used to encapsulate cells at physiological cell fractions.^[81]

2.4. Case Studies on Gel-Phase Bioink Materials

While there are numerous examples of sol-phase bioinks that undergo a postprinting crosslinking step, there have been relatively few demonstrations of dual-stage crosslinked materials (Table 2), that is, ink materials that are in the gel-phase both in the syringe and following printing. Here, we focus on such gel-phase bioinks, which are uniquely suited to maintain cell viability during the printing process, as described previously. For additional methods of bioink formation and printing strategies, we point the interested reader to several other excellent recent reviews.^[2,44,82]

Some of the first bioinks to be developed were based on alginate, a polysaccharide derived from brown seaweed that can be electrostatically crosslinked by divalent cations.^[83,84] As a single-material ink, alginate is uniquely suited to a dual-stage crosslinking approach because the degree of crosslinking can be modulated by varying cation concentration. For example, adding a small amount of calcium to alginate creates a weak, gel-phase ink that has been shown to prevent cell settling and reduce cell membrane damage during extrusion.^[85] Additional calcium can then be added postprinting (e.g., in the cell culture medium) as a second stage of crosslinking, which stiffens the final printed structure. This crosslinking strategy has been employed to print a variety of cell types, including neural progenitor cells (NPCs), which could be efficiently grown and expanded while maintaining their stem-like state within the printed alginate constructs.^[85,86] However, care must be taken to avoid using excess calcium to crosslink these materials as nonphysiological levels of calcium could be harmful to cells.^[87]

Alginate can also be combined with other materials to create dual-crosslinked bioinks with two distinct crosslinking mechanisms. To create a recombinant-protein alginate platform for injectable dual-crosslinked (RAPID) bioink, researchers tethered a proline-rich peptide (P) to an alginate backbone. When this P-modified alginate is mixed with an engineered protein (C7) that contains seven repeats of a complementary peptide (C), the P and C peptides spontaneously assemble into heterodimers.^[88] This molecular recognition of the two complementary peptide domains results in formation of a reversible, shear-thinning network with a relatively low storage modulus. Upon printing the ink into a calcium ion-rich bath, secondary electrostatic crosslinks reinforced the scaffold and increased the storage modulus of the gel more than 100-fold. The RAPID ink platform enabled patterning of multiple cell types that maintained their spatial organization over one week in culture. In another demonstration, alginate was mixed with gelatin methacryloyl (GelMA) and 4-arm poly(ethylene glycol)-tetraacrylate (PEGTA) to increase the cell-responsiveness of the bioink. Here, the alginate component of the blended bioink was first ionically crosslinked by calcium ions in the print cartridge, which improved the printability of the ink. Then the printed structure was irradiated with UV light such that the GelMA and PEGTA were covalently photocrosslinked. This technique

Table 2. Dual-stage crosslinked bioink materials.

Bioink material backbone	First stage crosslinking	Second stage crosslinking	Refs.
Alginate	Ionic (CaSO_4)	Ionic (CaCl_2)	[85]
	Ionic (CaCl_2)	UV irradiation	[107]
Alginate/collagen	Ionic (CaCl_2)	pH-mediated	[108]
Alginate/gelatin	Ionic (CaCl_2)	Genipin	[108]
	Ionic (CaCl_2)	UV irradiation	[108]
Alginate/recombinant polypeptide (RAPID)	Peptide–peptide interactions	Ionic (CaCl_2)	[20,88]
Carrageenan	Ionic (KCl)	UV irradiation	[109]
Chitosan/gelatin	Guest–host	Ionic and hydrogen bonds	[110]
Fibrinogen	PEG-SVA crosslinker	Enzymatic (thrombin)	[103]
Gelatin	PEG-SVA crosslinker	EDC/NHS crosslinking	[103]
	PEG-SVA crosslinker	UV irradiation	[103]
Gelatin/hyaluronic acid	DTT or PEG-8-SH	Visible light irradiation	[101]
	PEG-SVA crosslinker	UV irradiation	[111]
Gelatin/peptide amphiphiles	PEG-SVA crosslinker	Ionic (CaCl_2)	[103]
Hyaluronic acid	Guest–host	UV irradiation	[65]
	Enzymatic	Visible light irradiation	[112]
Hyaluronic acid/PNIPAM	Thermal	UV irradiation	[95]
Hyaluronic acid/recombinant polypeptide	Peptide–peptide interactions (“dock-and-lock”)	UV irradiation	[113]
	Hydrazone crosslinking	Thermal	[114]
Methylcellulose	Thermal	Visible light irradiation	[94]
Pectin	Ionic	UV irradiation	[115]
PNIPAM/recombinant polypeptide	Peptide–peptide interactions	Thermal	[116]
Silk	Metal–ligand coordination bonds	UV irradiation	[117]

was used to create highly organized vascular networks and supported the spreading and proliferation of encapsulated endothelial cells and MSCs.^[89]

Beyond ionic crosslinking, various other physical crosslinking mechanisms have been used to create gel-phase bioinks. In particular, supramolecular assembly through guest–host complexes has been widely explored for bioink development. These inks take advantage of the ability of guest–host complexes to disassemble upon application of a physical force and then reform once the force is removed, creating a hydrogel ink that is both shear-thinning and self-healing. In this case, the guest–host crosslinks serve as a single crosslinking mechanism to maintain the ink in the gel phase both in the syringe and after printing. In one example, hyaluronic acid (HA) was modified with either adamantine or β -cyclodextrin and then mixed to form a supramolecular hydrogel (Figure 2A). The mechanical properties of the bioink could be modulated by varying the degree of chemical modification, HA concentration, or ratio of guest–host molecules.^[65] However, while guest–host complexation was shown to be an effective first-stage crosslinking step, the dynamic nature of the crosslinks necessitated a second stage of crosslinking to improve long-term stability of the printed structures. Introducing additional photocrosslinkable methacrylate groups onto the HA backbone and then photopolymerizing the structure postprinting resulted in structures that were stable for one month and maintained their mechanical properties over time.^[90]

This strategy of combining a first stage of physical crosslinking with a second stage of covalent crosslinking initiated through UV or visible light is perhaps the most ubiquitous method to create dual-crosslinked materials.^[91–93] Several demonstrations have combined a first stage of thermal gelation with a secondary UV crosslinking step (Figure 2B).^[94–96] This strategy has also been used to print decellularized extracellular matrix (dECM) inks, which have the advantage of containing native bioactive and cell-adhesive domains.^[75,97] In the future, dECM inks could be tailored to create patient-specific constructs.^[71] Despite the popularity of photocrosslinking as a curing mechanism, there remain some concerns over cell toxicity in response to UV irradiation.^[98] Increasing UV exposure time has been shown to decrease cell viability, and this response was more pronounced in printed structures as compared to cast hydrogels, perhaps suggesting that the cells are already in a stressed state due to extrusion forces.^[43,99] Several methods to overcome this limitation have been developed, including using materials that have higher conversion rates of functional groups and thus can be crosslinked using shorter exposure times, materials that can be crosslinked by visible light, and printer nozzles that have been modified with a transparent capillary that allows for photocrosslinking as the material is extruded from the nozzle instead of bulk irradiation postprinting.^[92,100–102]

Alternatively, both stages of crosslinking can be facilitated by covalent crosslinking chemistries without the use of light.

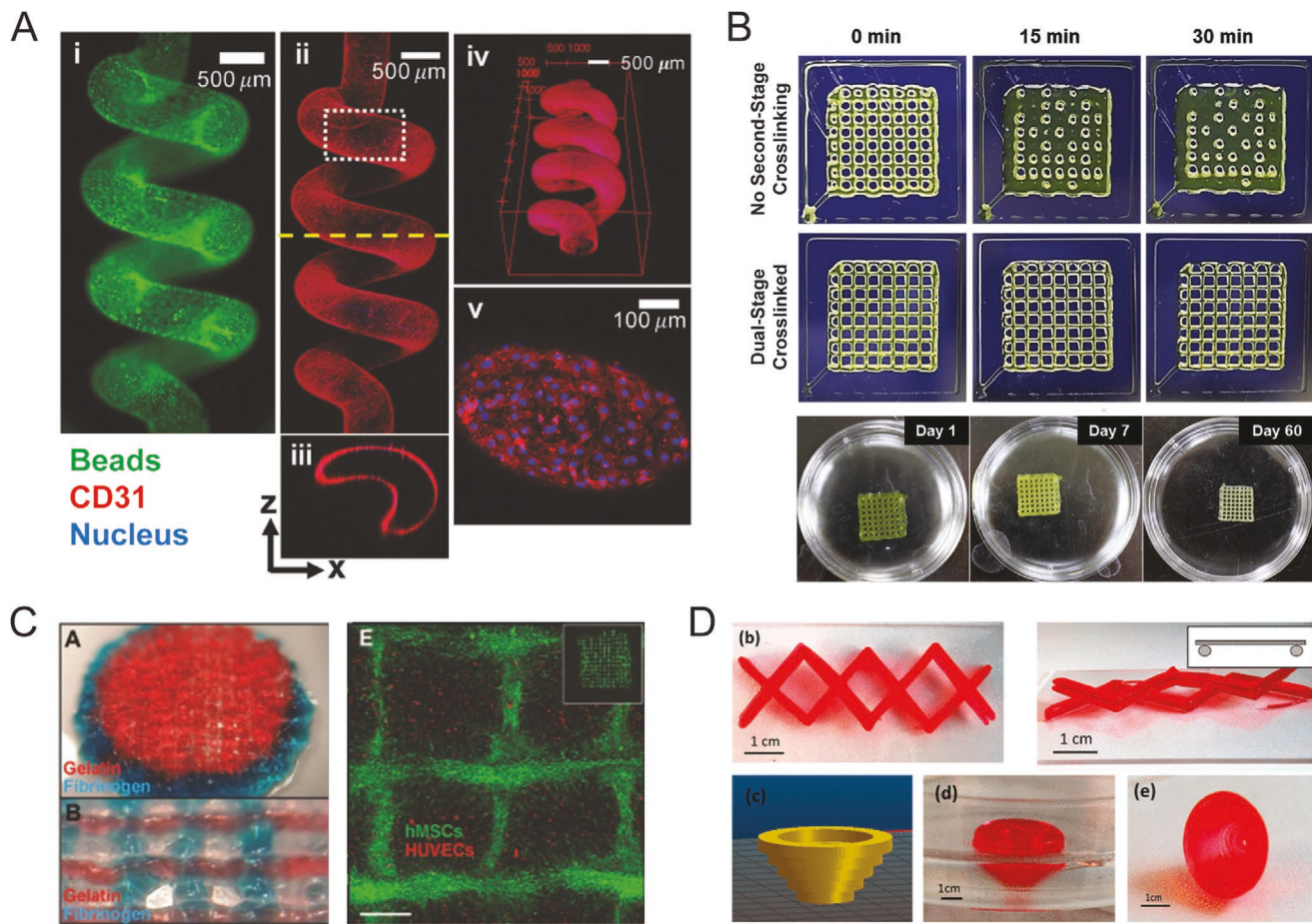


Figure 2. Dual-stage crosslinked bioprinted structures. A) A shear-thinning and self-healing bioink based on supramolecular assembly through guest-host complexes allows for continuous printing in any direction of 3D space and seeding with endothelial cells. Reproduced with permission.^[106] Copyright 2018, Wiley-VCH. B) Dual-crosslinked tyramine-modified methylcellulose 3D printed lattices retained structural stability up to 60 days, while printed constructs that did not undergo a second stage of crosslinking (exposure to light) and thus were only thermally crosslinked steadily collapsed within 30 min. Reproduced with permission.^[94] Copyright 2020, Elsevier. C) Dual-stage crosslinked PEGX-gelatin (red) and PEGX-fibrinogen (blue) inks were printed together and then covalently crosslinked by a small molecule. This facilitated multimaterial and multicell type printing with HUVECs (CellTracker Red) and hMSCs (CellTracker Green). Reproduced with permission.^[103] Copyright 2015, Wiley-VCH. D) A polymerizable shear-thinning Pluronic F127-dimethacrylate hydrogel ink was mixed with an initiator (ammonium persulfate, APS) and then printed into a support gel containing a catalyst (tetramethylethylenediamine, TMEDA). After removal from the bath, complex printed structures such as an inverted cone retained their shape without collapsing. Reproduced with permission.^[105] Copyright 2017, American Chemical Society.

In one example, a small number of PEGX crosslinkers (where X = succinimidyl valerate, SVA, which can react with amines) were added to amine-containing polymers, creating a lightly crosslinked, soft hydrogel ink that could be easily extruded (Figure 2C).^[103] To increase the stiffness and stability of the printed structure, another, secondary covalent crosslinking step was employed in which a solution of the same PEGX crosslinkers was added on top of the printed structure. These two-stage crosslinked materials provided longer term stability and increased cell viability as compared to printing inks with a greater number of first-stage crosslinks without the secondary crosslinking step. A follow-up study also expanded the identity of the PEGX functional groups to include more cytocompatible crosslinking chemistries (e.g., thiol-based Michael type addition and the bioorthogonal inverse electron demand Diels–Alder reaction).^[104] In another example, a polymerizable shear-thinning Pluronic F127-dimethacrylate hydrogel ink was mixed

with an initiator (ammonium persulfate, APS) and then printed into a support gel containing a catalyst (tetramethylethylenediamine, TMEDA). When the printed gel came into contact with the support gel containing the catalyst, free radicals were generated and the hydrogel ink was polymerized via a vinyl addition, crosslinking the printed structure (Figure 2D). Unlike photopolymerization, this catalyst-induced polymerization method was effective for printing inks with increased opacity since it was not dependent on light penetration through the construct.^[105]

These examples demonstrate how dual-stage crosslinked materials can be used to make bioinks that are both printable and stable for long-term culture. First-stage crosslinking to create gel-phase inks improves cell viability and filament formation, while second-stage crosslinking stiffens the construct and allows for the final mechanical properties of the structure to be tuned independently of the rheological properties needed for printing. In the future, we expect that the number of materials

available for bioprinting will greatly expand and that bioinks will be made more customizable. This will be facilitated by creating new crosslinking strategies and incorporating additional chemistries into bioink design that have already been developed for hydrogels used in tissue engineering.

3. Future Perspective: Bioprinted Constructs as Living, Composite Materials

While hydrogel design for 3D bioprinting has largely focused on material properties that allow for suitable printing, this approach often fails to acknowledge that a bioink is by definition composed of both a nonliving component (the polymer) and living component (the cells), making a printed construct an active, dynamic material after bioprinting. The geometric and biological transformations of the material are governed by interactions of the hydrogel component of the bioink with the cells embedded within the construct and with the external environment in which the construct is cultured. Engineering hydrogels for 3D bioinks with consideration to cells as an intrinsic component of the printed “material” will advance the field of 3D bioprinting toward greater biofunctionality through control of the postprinting evolution of the living construct.

For bioprinted constructs to serve as in vitro models of natural tissue or implants to regenerate functionality of a damaged tissue in the body, the material must mature to adopt a form and function more similar to native, functional tissue.^[2,118] Thus far, only a small fraction of the bioprinting literature has demonstrated high functionality in bioprinted constructs that closely recapitulates tissues or organs. In this section, we discuss facets of 3D bioprinted construct evolution that may present challenges or unexpected material properties if not considered, but that also provide opportunities for advanced hydrogel design toward enhanced geometric complexity and biological function. These include effects of the cells on the polymer, the polymer on the cells, and the external environment on both components of the composite material (Figure 3).

3.1. Density and Distribution of Cells within Prints

The rate of tissue maturation is greatly affected by the density and distribution of cells within the bioprinted construct as cells remodel the surrounding hydrogel. Hydrogels that allow for cell-mediated remodeling unsurprisingly experience accelerated remodeling with higher cell densities.^[119,120] Remodeling occurs through cell adhesion, contraction, degradation of the initial hydrogel material, and deposition of new ECM.^[121] The initial cell density and distribution within the bioprinted construct are dependent on the composition of the bioink and the printing process. In some cases, it is not possible to print hydrogel-based bioinks with initial cell densities higher than a certain threshold, since the presence of cells within the bioink may alter the rheological properties of the bioink and interfere with the hydrogel network formation or crosslinking steps.^[122,123] During the cell culture period postprinting, however, the density of cells within the bioprinted construct may increase from this initial state due to cell proliferation.^[124] Furthermore, it is

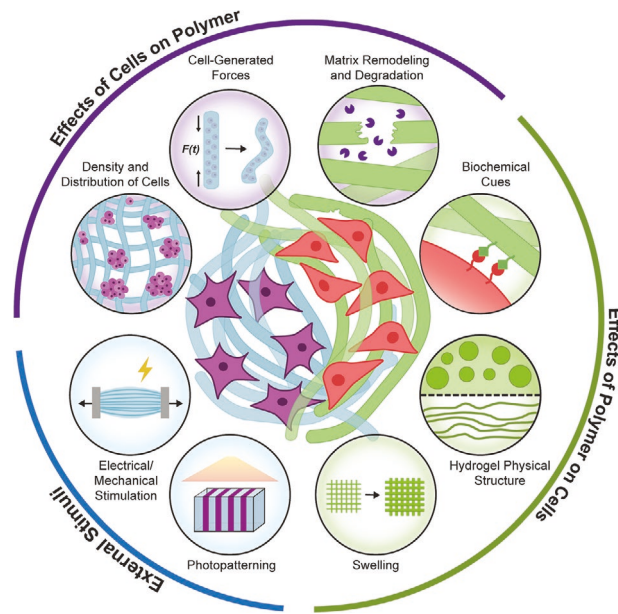


Figure 3. Postprinting, the living construct will change and “mature” over time, which can be influenced by material design choices. As bioprinted constructs are active, dynamic hydrogels, they will evolve over time as the polymer component interacts with the cellular component. In the future, developing customizable bioink polymers for multiple cell types that guide polymer–cell interactions postprinting will enable fabrication of more complex tissue types. The embedded cells can act on the polymer through cell-generated forces and matrix remodeling/degradation, where the rate of matrix remodeling is dependent on the density and distribution of cells within the structure. Conversely, the polymer can also affect cellular behavior through biochemical cues such as growth factors, the presence of cell-adhesive sites, the mechanical properties and structural features of the material that influence mechanotransduction, and polymer swelling. Finally, external stimuli such as electrical stimulation, mechanical stimulation, and photopatterning can be used to accelerate the maturation of printed hydrogels into more tissue-like constructs.

possible to seed additional cells on the construct postprinting or print directly into a bath of cells in order to avoid the challenges associated with prohibitively high cell densities within the bioink during extrusion.^[125]

The distribution of cells within the construct is not always entirely homogenous during printing and can evolve due to cell proliferation and migration, which in turn changes the construct properties postprinting.^[126] Cells communicate via signaling molecules or cell–cell contacts to self-organize and adjust their position within the matrix, influencing the form of the construct.^[127,128] For example, spheroids of cells and biomaterial may merge together into a continuous structure over time,^[127,128] while a defect in the construct shape may grow over time rather than heal.^[129] In addition to changing the construct shape, a numerical modeling study on the effect of proliferation on cellular distributions within a hydrogel—randomly distributed or arranged in either multiple “edge clusters” or a single “central cluster”^[130–132]—has demonstrated that hydrogels with clustered cells have a notably different modulus than those with a random distribution of cells.^[124] The overall modulus of the construct, therefore, has the potential to evolve over time as the density and distribution of cells change, and reporting only

the modulus of a bioink polymer alone may not be representative of the material properties during culture.

3.2. Cell-Generated Forces

Cells dynamically interact with their surrounding matrix and generate traction forces that act upon the hydrogel macromolecules within a printed construct. When cells form focal adhesions with the ECM, transmembrane integrins transmit mechanical force by pulling on the ligands.^[133] The amount of traction generated at focal adhesions is specific to each cell type; cardiomyocytes, for example, are highly contractile.^[134] Since hydrogels may exhibit viscoelastic behavior, cell-generated tension is sometimes able to dissipate through the hydrogel due to stress-relaxation of the polymer network. In some cases, however, stress gradients from these cellular contractile forces may cause mechanical instabilities and construct deformation. For example, cell-generated forces within microbeams that were 3D bioprinted into a support bath of microgels caused evolution of their structure. Depending on the cell density, hydrogel concentration in the bioink, construct size, and material properties of the surrounding support gel, a range of construct changes were observed due to cell-generated forces over time, including buckling, axial contraction, failure, or total static stability (Figure 4).^[135]

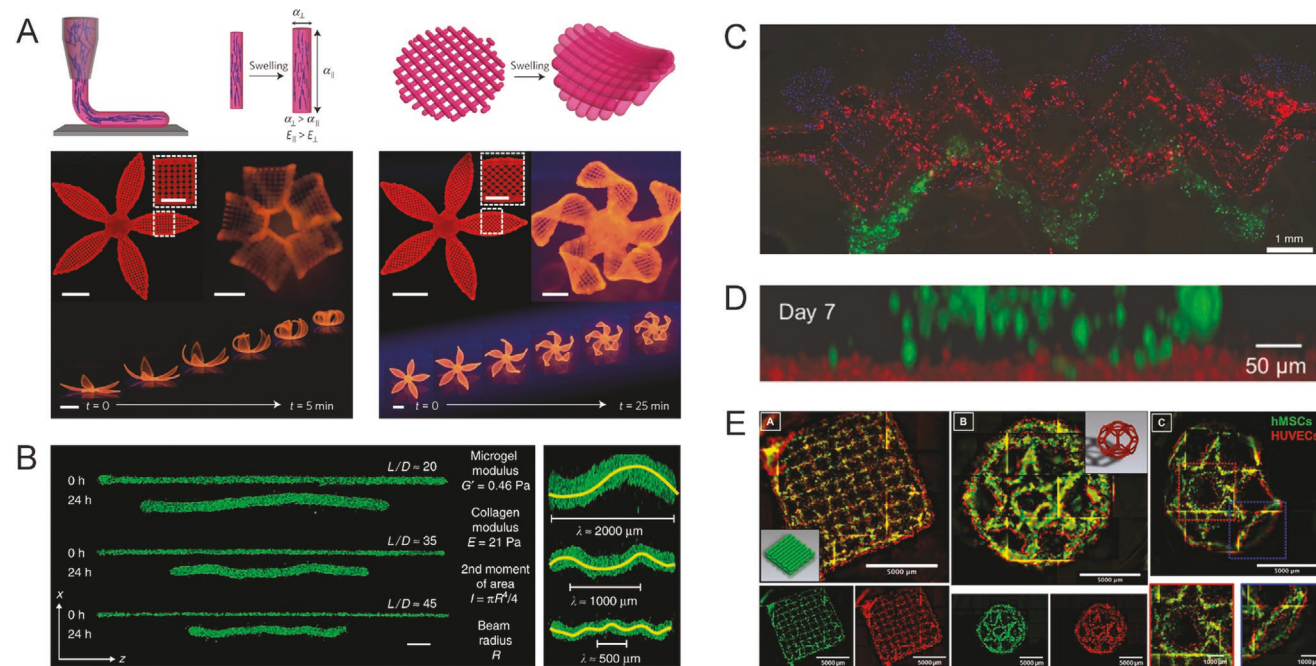


Figure 4. Properties of the hydrogel material may be engineered to form geometrically complex structures and cell patterns. A) Cellulose nanofibers within a hydrogel ink align in the direction of printing due to shear forces during extrusion, leading to anisotropic mechanical and swelling properties that allow for controllable, dynamic changes in morphology. Scale bars: 5 mm; inset = 2.5 mm. Reproduced with permission.^[143] Copyright 2016, Springer Nature. B) Internal, cell-generated contractile forces cause undulation of printed microbeams over 24 h. Buckling behavior is controlled by the print filament diameter and the moduli of the bioink material and gel-based support bath. Reproduced under the terms of the CC-BY 4.0 License.^[135] Copyright 2019, The Authors, Published by Springer Nature. C) A heterogeneous print demonstrates patterning of three different cell types (10T1/2 fibroblasts, blue; HNDFs, green; HUVECs, red) in a single-tissue construct. Reproduced with permission.^[21] Copyright 2014, Wiley-VCH. D) Printed cell layers (hASCs, red; 3T3 cells, green) retain their spatial fidelity over 7 days. Reproduced with permission.^[88] Copyright 2016, Wiley-VCH. E) Multiple cell types (hMSCs, green; HUVECs, red) may be encapsulated within a single bioink that is printed into 3D custom-shaped constructs. Reproduced with permission.^[144] Copyright 2020, American Chemical Society.

For increased control over geometric changes, the construct could be engineered to respond to cell-generated forces in a predetermined way. For instance, when deformation is not desired, increasing the polymer concentration in the bioink or the modulus of the surrounding supporting gel decreases the magnitude of changes to the construct shape or stability attributed to cellular forces.^[135] On the other hand, it may be possible to amplify cell forces on the hydrogel matrix in order to alter the global geometry, for instance, by controlling cell-adhesive ligand densities and locations within the hydrogel construct. Cell-laden microplates, for example, have been demonstrated to roll into a cylinder or fold into a cube due to cell-generated forces exerted on the surface of the constructs.^[136] From the understanding of geometric changes induced by cell-generated forces in hydrogel films and simple geometries, the internal forces imposed by cells onto their surrounding matrix could be leveraged in more complex structures in bioprinting.

Finally, the forces that cells impose onto their surroundings not only influence the shape of the construct but also cellular behavior, particularly when anisotropic tensions are created. For example, cells react to self-generated tension by elongating themselves and depositing ECM in alignment with the direction of the tension.^[137] Therefore, creating anisotropic tensions within a printed construct may guide cell behavior and the properties of deposited matrix as the material matures.

3.3. Matrix Remodeling and Degradation

In many cases, the original hydrogel component of the bio-printed construct ideally degrades over time and is gradually replaced by the ECM components deposited by cells. The hydrogel material in the construct may undergo degradation mediated by cells or external factors in their environment. For example, cells can degrade hydrogels that contain enzymatic cleavable sequences in the polymer backbone or crosslinks. During enzymatic degradation, proteases secreted from cells degrade their surrounding matrix, allowing for cell spreading, dynamic engagement with the surrounding ECM, and volume expansion upon proliferation. This cell-mediated matrix degradation and remodeling has the advantage of spatiotemporal synchronization with tissue generation. Enzyme kinetics can be used (e.g., with Michaelis–Menten models) to predict and tune the degradation profile. An important consideration is the balance between the printed construct having sufficient mechanical strength and integrity to maintain its printed structure while still allowing cells to remodel the matrix. To achieve this, an alternate approach is to design hydrogels with a combination of adaptable and permanent crosslinks, as has been demonstrated by bioprints with dynamic covalent hydrazone linkages along with a photocrosslinkable interpenetrating network.^[76] The permanent crosslinks provide structural integrity to the hydrogel, while adaptable crosslinks facilitate cell-mediated matrix remodeling for proliferation, migration, and tissue formation. The relative amounts of crosslinker types could be tunable to optimize the balance between mechanical stability and cell remodeling of the material.

Biodegradable hydrogel materials often also degrade over time under physiological conditions in culture medium due to the erosion of physical crosslinks or the hydrolysis of ester, anhydride, or amide bonds.^[138] Hydrogels with higher degrees of crosslinking and stronger physical bonds tend to erode more slowly. In the case of this nonenzymatic degradation, the presence of cells can also slow the overall degradation rate of the hydrogel-based construct compared to acellular hydrogels because of their ECM deposition and matrix remodeling.^[139] Although the cleavage of bonds due to hydrolysis is controllable and predictable from information about the initial polymer network such molecular weight, crosslinking, and hydrolysis kinetics, hydrolytic degradation cannot generally be regulated or altered in real-time after gel formation.^[140] Alternatively, a photo-degradable functionality incorporated into the backbone of a PEG-based hydrogel could be cleaved by spatiotemporally controlled exposure to light.^[141,142] This ability to remotely manipulate the material properties of the hydrogel in real-time allowed for local degradation of the hydrogel to create channels and arbitrary features at specific timepoints.^[141] Degradation gradients were also created through the material and increased cell spreading was observed in regions of the hydrogel with greater degradation.^[142] Coupled with the initial geometric complexity already feasible with 3D bioprinting, externally controlled local degradation would allow for time-dependent changes to the geometry of the construct in order to either probe fundamental biological questions or control the dynamic relationship between cells and the structural properties of their surrounding matrix.

3.4. Promoting Biofunctionality

3.4.1. *Multibioink Prints*

To date, the majority of 3D bioprinting demonstrations have used a single type of cell and material to formulate the bioink for a printed construct. In contrast, native tissues and organs have distinct spatial arrangements of different cell types, matrix compositions, and biochemical signals. The ability to pattern multiple types of cells using 3D bioprinting will be a significant advancement in the field of tissue engineering toward replicating anatomic features of native tissues for *in vitro* models or implantation. In one example, a multinozzle bioprinter patterned separate inks containing osteoblasts and chondrocytes to mimic the interface between bone and cartilage for osteochondral tissue engineering.^[145] In another example, dual cell-laden bioinks of chondrocytes and bone-marrow-derived mesenchymal cells printed and subcutaneously implanted in mice resulted in more pronounced neocartilage formation *in vivo* than bioprints with only chondrocytes.^[146] While these studies have demonstrated the potential of bioprinting with two or more cell types, there are several challenges associated with printing multiple bioinks into a single construct. Crosslinking mechanisms may not be compatible between ink materials, and the matrix requirements for the cells may be different. For multi-ink structures, cohesion between the two printed materials is also a key requirement. One strategy to achieve multi-ink cohesion is to employ a universal crosslinking strategy for all materials in one print. A recent demonstration of a Universal Orthogonal Network (UNION) crosslinking platform employed a small molecule crosslinker loaded in the support bath that diffused into bioinks conjugated with bioorthogonal functional groups. This approach allowed for multiple materials to be crosslinked using a single mechanism into a cohesive, multimaterial print.^[81] Furthermore, the materials within each bioink should be tailored to fit the needs of that cell type. Developing customizable and compatible bioink materials for multiple cell types will accelerate the geometric complexity and heterogeneity that can be introduced into bioprinted constructs for better biomimicry.

3.4.2. *Biochemical Features*

Within the tissue engineering field, biofunctionality is often achieved by incorporating peptide motifs for cell-adhesive ligands into the hydrogel.^[85,147] Ligands can be covalently bound to a polymer, incorporated into the polymer backbone, adsorbed to the material, or added as an interpenetrating network. The tripeptide RGD, found in fibronectin, is commonly used as a minimal integrin-binding sequence since most cells have a receptor that binds to it, but other peptide sequences such as the laminin-derived sequences YIGSR and IKVAV and the collagen-derived GFOGER and DGEA have also been used both alone and in conjunction with other ligands.^[148] The concentration, affinity, and mobility of ligands affect cell morphology and gene expression^[149,150] and therefore could be optimized for different cell types within each bioink.^[151–153] By identifying and including biochemical signals crucial to the desired cell

type and function in the hydrogel that encapsulates the cells, the biological functionality of the bioprinted construct can be enhanced while also expanding the types of cells that can be used in bioprinting.

Growth factors, which can also be specific to each cell and tissue type, can be tethered to the hydrogel network or solubilized in the medium to promote the desired cell growth or function. MSCs and endothelial cells have been demonstrated to preferentially migrate into gradients of certain growth factors.^[106,154,155] For example, angiogenic sprouting was observed from a 3D printed microchannel of endothelial cells toward increasing concentrations of soluble angiogenic growth factors within the support gel.^[106] Recently, the ability to print with distinct growth factor patterns and release times was demonstrated by incorporating growth factor-loaded nanoparticles into the bioinks. The degree of angiogenesis was dependent on the spatial presentation of VEGF and BMP-2, with enhanced angiogenesis for gradients of growth factors over a homogeneous presentation.^[155] 3D bioprinting is uniquely positioned to create patterns with control over the type, concentration, and location of growth factors, which could aid in regenerative medicine applications.

3.4.3. Hydrogel Physical Structure

In addition to the importance of the biochemical features of the hydrogel, cell behavior such as the differentiation of stem cells or velocity of migration depends on the physical properties and microstructure of the hydrogel.^[53,156] Tissues *in vivo* contain complex, tissue-specific hierarchical structures such as microscale topography, porosity, and fibril alignment that provide signals to cells.^[157] Hydrogels can be designed to incorporate microscale features such as fiber-like geometries and microscale porosity to guide cell functions and movement. For example, oriented fibers stimulate anisotropy in cell elongation and migration.^[158,159] During bioprinting, shear and extensional forces imparted on the bioink as it is extruded through the nozzle can align fibers in the hydrogel depending on the level of shear stress.^[26] In addition, hydrogels with microscale porosity, such as granular hydrogels, have demonstrated enhanced ability for cellular infiltration compared to nanoporous hydrogels and can be used as the bioink material when increased cell migration and rearrangement is desired.^[160–162]

The evolution of the macroscale structure of the construct is often transformed due to swelling of the hydrogels, since constructs are cultured in aqueous solutions to keep cells hydrated. Swelling behavior of a bioprint is governed by the inherent solubility of the polymer, crosslinking density, and heterogeneity of the construct.^[86,87] For example, the commonly used hydrogel PEG swells significantly due to its strongly hydrophilic, water-soluble nature, while the amphiphilic polymer Pluronic (a PEG–polypropylene glycol (PPG)–PEG triblock polymer) has limited water sorption due to its hydrophobic component.^[163] The swelling ratio of hydrogels also decreases with increasing degree of crosslinking; while crosslinking density can be modulated to control swelling, the rheological properties of the hydrogel are simultaneously affected.^[164] In heterogeneous

bioprints with multiple materials or complex geometries, localized or anisotropic swelling may lead to significant changes in geometry after printing. These temporal changes to the bioprinted construct can be harnessed to create so-called “4D” bioprinted materials.

In particular, many tissues in the human body contain curved or folded regions, such as tubular ducts in mammary glands that influence breast cancer cell behavior due to strain, curvature, and confinement effects.^[165] For creating complex, curved geometries, hydrogel constructs have been designed that swell anisotropically upon exposure to water to significantly transform in shape. For example, flat PEG-based bilayers with two different molecular weights experience differential swelling in water that induced spontaneous curvature of the bilayers.^[166,167] By changing the crosslinking pattern with photolithography, the bilayers self-folded into a variety of geometries including spherical capsules, helices, and cylinders.^[166] In another approach to achieve complex geometries of multilayered hydrogels through anisotropic swelling, a composite ink of cellulose fibrils embedded within an acrylamide matrix was used.^[143] During extrusion, the cellulose fibrils experienced shear forces that aligned them in the direction of printing. The printed filaments, therefore, had anisotropic stiffnesses and preferentially swelled in the transverse direction. By printing layers of filaments in different patterns, the direction and extent of curvature of the multilayered construct was controlled to create intricate, flower-like shapes upon swelling.^[143] Although cells were not encapsulated in the ink in this example, the theoretical frameworks that guided the printing patterns for controlled, anisotropic swelling could be applied for cell-laden bioinks. The design of bioinks that can be printed in a flat print path but spontaneously swell into a desired shape in aqueous cell culture medium allows for high resolution structures with delicate geometric features.

3.5. Accelerated Maturation via External Stimuli

While the methods to improve biological functionality of bioprinted constructs described thus far have focused on material design parameters within the construct, the maturation of hydrogels and cells into more tissue-like constructs has also been accelerated by the application of physiologically relevant external stimuli. For cartilage tissue engineering, mechanical stimulation of constructs in compression increases the amount of ECM synthesis and enhances chondrocyte differentiation.^[168] In another example, *in vitro* models of cardiac tissue have been observed to benefit from electrical stimulation that promotes differentiation toward a cardiomyocyte lineage and induces synchronization of beating.^[169,170] Finally, as discussed in Section 3.3, spatiotemporally controlled degradation of a hydrogel has been achieved with photopatterning.^[141,142] Further development of bioink materials that enable these types of post-printing external stimuli are expected to lead to more “mature” artificial tissues. For example, the use of injectable, conductive hydrogels as bioinks coupled with the postprinting application of external electrical stimulation would be a tailored strategy for cells that require the conduction of electrical signals for optimal functionality. By considering the physiological conditions

Table 3. A selection of in vitro assays to characterize the living component of 3D bioprinted materials. These analytical techniques are commonly used in biomaterials research.

Outcome variable	Assays
Viability	Live/dead stain
Proliferation	PicoGreen; Bromodeoxyuridine (BrdU) stain
Metabolism	Tetrazolium dye (e.g., MTT); Alamar Blue
Morphology	Confocal microscopy
Signaling	Agonist/antagonist studies; immunocytochemistry
Gene activation	Gene array; quantitative reverse transcription polymerase chain reaction (qRT-PCR); next generation sequencing (NGS)
Protein expression	Western blot; immunocytochemistry
Protein secretion	Enzyme-linked immunosorbent assay (ELISA)

relevant for the target tissue type, bioprinted constructs may mature to more closely resemble native tissue.

In summary, to advance the achievable complexity of 3D bioprinted constructs for increased biomimicry, the postprinting evolution and “final” properties of a hydrogel-based construct can be governed using a wealth of knowledge from the fields of polymer chemistry and tissue engineering. Considering a bioprinted construct as a living, composite material with polymer and cells as intrinsic elements requires the evolution of both components to be characterized for a comprehensive understanding of the material. For example, in addition to quantification of the physical and mechanical properties of the print over time, the living component of the 3D bioprinted construct should be assessed with assays commonly referred to in the tissue engineering community as characterization of “cells in gels” (Table 3). In recent years, computational and theoretical frameworks are also being developed and validated experimentally to predict and understand the interactions that biomaterials have with cells and the external environment during culture.^[124] By predicting the structural and biological evolution of the construct over time, the relevant initial parameters of the 3D bioprinting process—including the design of the hydrogel materials—can be engineered to better control the ultimate geometric structure and biological function of the bioprinted construct.

4. Conclusion

Gel-phase materials have demonstrated great potential for use in 3D bioprinting as bioinks. Early demonstrations of 3D bioprinting often optimized bioink materials for printability, with the tradeoff that they suffered from challenges maintaining cell viability and biological functionality. Advanced hydrogels are now being developed to support cells during all stages of the printing process: in the print cartridge, as the bioink is extruded through the nozzle, during any material crosslinking steps, and as the printed construct is being cultured. In this way, hydrogels can provide structural support during and after printing, as well as biological and mechanical cues to promote cellular function. Looking forward, the design of new, more

advanced bioinks will benefit from the previous decades of biomaterials research that has sought to understand and optimize the biochemical and biomechanical signals present in hydrogels. These material properties should be tailored to the cell type, tissue, or organ of interest, and must be engineered with consideration to the final application of the construct, whether it be for in vitro models or in vivo transplantation. There is also a growing appreciation that bioprinted constructs are active, living materials containing both an acellular (polymer) component and a cellular component. Thus, the properties of the final construct will evolve over time due to reciprocal cell–material interactions as well as influences from the external environment; this evolution can be leveraged for dynamic or “4D” prints. Future work in the field will improve upon the bioink material’s ability to guide cell behavior by better mimicking physiological features, by adding cell-specific biochemical and mechanical features, and by increasing complexity and heterogeneity with multibioink constructs. Altogether, the use of advanced hydrogel materials as bioinks should propel forward the 3D bioprinting field toward greater biological complexity and function.

Acknowledgements

S.M.H. and L.G.B. contributed equally to this work. The authors thank C. D. Lindsay, A. J. Seymour, and S. Shin for helpful conversations about this manuscript. The authors acknowledge funding support from the National Science Foundation (DMR 2103812, CBET 2033302, and DMR 1808415) and the National Institutes of Health (R21 HL138042, R21 NS114549, R01 HL142718, R01 EB027171, R01 HL151997, and R01 EB027666). S.M.H. acknowledges funding from an NIH NRSA predoctoral fellowship (F31 EY030731) and a Stanford Bio-X Interdisciplinary Graduate Fellowship. L.G.B. acknowledges funding from an NSF Graduate Research Fellowship.

Conflict of Interest

The authors declare no conflict of interest.

Keywords

biofabrication, bioink, bioprinting, hydrogel, regenerative medicine, tissue engineering

Received: May 15, 2021

Revised: September 15, 2021

Published online:

- [1] D. Chimene, R. Kaunas, A. K. Gaharwar, *Adv. Mater.* **2020**, *32*, 1902026.
- [2] R. Levato, T. Jungst, R. G. Scheuring, T. Blunk, J. Groll, J. Malda, *Adv. Mater.* **2020**, *32*, 1906423.
- [3] A. Schwab, R. Levato, M. D’Este, S. Piluso, D. Eglin, J. Malda, *Chem. Rev.* **2020**, *120*, 11028.
- [4] W. Sun, B. Starly, A. C. Daly, J. A. Burdick, J. Groll, G. Skeldon, W. Shu, Y. Sakai, M. Shinohara, M. Nishikawa, J. Jang, D. W. Cho, M. Nie, S. Takeuchi, S. Ostrovidov, A. Khademhosseini,

- R. D. Kamm, V. Mironov, L. Moroni, I. T. Ozbolat, *Biofabrication* **2020**, *12*, 022002.
- [5] E. B. Hunziker, T. M. Quinn, H. J. Häuselmann, *Osteoarthritis Cartilage* **2002**, *10*, 564.
- [6] T. M. Quinn, H. J. Häuselmann, N. Shintani, E. B. Hunziker, *Osteoarthritis Cartilage* **2013**, *21*, 1904.
- [7] P. G. Braunschweiger, L. Schiffer, P. Furmanski, *Magn. Reson. Imaging* **1986**, *4*, 285.
- [8] A. Blouin, R. P. Bolender, E. R. Weibel, *J. Cell Biol.* **1977**, *72*, 441.
- [9] P. M. Gullino, F. H. Grantham, S. H. Smith, *Cancer Res.* **1965**, *25*, 727.
- [10] K. M. Donahue, R. M. Weisskoff, D. J. Parmelee, R. J. Callahan, R. A. Wilkinson, J. B. Mandeville, B. R. Rosen, *Magn. Reson. Med.* **1995**, *34*, 423.
- [11] H.-I. Peterson, *Tumor Blood Circulation: Angiogenesis, Vascular Morphology and Blood Flow of Experimental and Human Tumors*, CRC Press, Boca Raton, FL **2020**.
- [12] N. B. Everett, B. Simmons, E. P. Lasher, *Circ. Res.* **1956**, *4*, 419.
- [13] F. A. Sreter, G. Woo, *Am. J. Physiol.* **1963**, *205*, 1290.
- [14] J. Groll, J. A. Burdick, D. W. Cho, B. Derby, M. Gelinsky, S. C. Heilshorn, T. Jüngst, J. Malda, V. A. Mironov, K. Nakayama, A. Ovsianikov, W. Sun, S. Takeuchi, J. J. Yoo, T. B. F. Woodfield, *Biofabrication* **2019**, *11*, 013001.
- [15] S. Derakhshanfar, R. Mbeleck, K. Xu, X. Zhang, W. Zhong, M. Xing, *Bioact. Mater.* **2018**, *3*, 144.
- [16] S. V. Murphy, A. Atala, *Nat. Biotechnol.* **2014**, *32*, 773.
- [17] C. F. Guimarães, L. Gasperini, A. P. Marques, R. L. Reis, *Nat. Rev. Mater.* **2020**, *5*, 351.
- [18] D. T. Butcher, T. Alliston, V. M. Weaver, *Nat. Rev. Cancer* **2009**, *9*, 108.
- [19] N. E. Fedorovich, I. Swennen, J. Girones, L. Moroni, C. A. van Blitterswijk, E. Schacht, J. Alblas, W. J. A. Dhert, *Biomacromolecules* **2009**, *10*, 1689.
- [20] K. Dubbin, A. Tabet, S. C. Heilshorn, *Biofabrication* **2017**, *9*, 044102.
- [21] D. B. Kolesky, R. L. Truby, A. S. Gladman, T. A. Busbee, K. A. Homan, J. A. Lewis, *Adv. Mater.* **2014**, *26*, 3124.
- [22] C. T. S. Wong Po Foo, J. S. Lee, W. Mulyasasmita, A. Parisi-Amon, S. C. Heilshorn, *Proc. Natl. Acad. Sci. USA* **2009**, *106*, 22067.
- [23] B. A. Aguado, W. Mulyasasmita, J. Su, K. J. Lampe, S. C. Heilshorn, *Tissue Eng., Part A* **2012**, *18*, 806.
- [24] G. G. Galbraith, R. Skalak, S. Chien, *Cell Motil. Cytoskeleton* **1998**, *40*, 317.
- [25] C. Yan, M. E. MacKay, K. Czynnemek, R. P. Nagarkar, J. P. Schneider, D. J. Pochan, *Langmuir* **2012**, *28*, 6076.
- [26] H. Kim, J. Jang, J. Park, K.-P. Lee, S. Lee, D.-M. Lee, K. H. Kim, H. K. Kim, D.-W. Cho, *Biofabrication* **2019**, *11*, 35017.
- [27] B. D. Olsen, J. A. Kornfield, D. A. Tirrell, *Macromolecules* **2010**, *43*, 9094.
- [28] Y. Zhao, Y. Li, S. Mao, W. Sun, R. Yao, *Biofabrication* **2015**, *7*, 045002.
- [29] K. Y. Lee, D. J. Mooney, *Chem. Rev.* **2001**, *101*, 1869.
- [30] B. M. Baker, C. S. Chen, *J. Cell Sci.* **2012**, *125*, 3015.
- [31] J. A. Burdick, W. L. Murphy, *Nat. Commun.* **2012**, *3*, 1269.
- [32] J. M. Unagolla, A. C. Jayasuriya, *Appl. Mater. Today* **2020**, *18*, 100479.
- [33] B. D. Ratner, S. J. Bryant, *Annu. Rev. Biomed. Eng.* **2004**, *6*, 41.
- [34] G. Gillispie, P. Prim, J. Copus, J. Fisher, A. G. Mikos, J. J. Yoo, A. Atala, S. J. Lee, *Biofabrication* **2020**, *12*, 022003.
- [35] A. Ribeiro, M. M. Blokzijl, R. Levato, C. W. Visser, M. Castilho, W. E. Hennink, T. Vermonden, J. Malda, *Biofabrication* **2017**, *10*, 14102.
- [36] L. Ouyang, R. Yao, Y. Zhao, W. Sun, *Biofabrication* **2016**, *8*, 35020.
- [37] J. M. Lee, W. L. Ng, W. Y. Yeong, *Appl. Phys. Rev.* **2019**, *6*, 11307.
- [38] H. Rastin, R. T. Ormsby, G. J. Atkins, D. Losic, *ACS Appl. Bio Mater.* **2020**, *3*, 1815.
- [39] V. H. M. Mouser, F. P. W. Melchels, J. Visser, W. J. A. Dhert, D. Gawlitza, J. Malda, *Biofabrication* **2016**, *8*, 035003.
- [40] C. C. Chang, E. D. Boland, S. K. Williams, J. B. Hoying, *J. Biomed. Mater. Res., Part B* **2011**, *98B*, 160.
- [41] A. Abbadessa, M. M. Blokzijl, V. H. M. Mouser, P. Marica, J. Malda, W. E. Hennink, T. Vermonden, *Carbohydr. Polym.* **2016**, *149*, 163.
- [42] F. Pati, J. Jang, D. H. Ha, S. Won Kim, J. W. Rhee, J. H. Shim, D. H. Kim, D. W. Cho, *Nat. Commun.* **2014**, *5*, 3935.
- [43] C. Colosi, S. R. Shin, V. Manoharan, S. Massa, M. Costantini, A. Barbutta, M. R. Dokmeci, M. Dentini, A. Khademhosseini, *Adv. Mater.* **2016**, *28*, 677.
- [44] J. Malda, J. Visser, F. P. Melchels, T. Jüngst, W. E. Hennink, W. J. A. Dhert, J. Groll, D. W. Hutmacher, *Adv. Mater.* **2013**, *25*, 5011.
- [45] A. Malkin, A. Y. Malkin, *Rheology Fundamentals*, ChemTec Publishing, Scarborough, Canada **1994**.
- [46] J. M. Townsend, E. C. Beck, S. H. Gehrke, C. J. Berkland, M. S. Detamore, *Prog. Polym. Sci.* **2019**, *91*, 126.
- [47] W. Schuurman, P. A. Levett, M. W. Pot, P. R. van Weeren, W. J. A. Dhert, D. W. Hutmacher, F. P. W. Melchels, T. J. Klein, J. Malda, *Macromol. Biosci.* **2013**, *13*, 551.
- [48] K. Nair, M. Gandhi, S. Khalil, K. C. Yan, M. Marcolongo, K. Barbee, W. Sun, *Biotechnol. J.* **2009**, *4*, 1168.
- [49] K. F. Freed, S. F. Edwards, *J. Chem. Phys.* **1974**, *61*, 3626.
- [50] L. Aulisa, H. Dong, J. D. Hartgerink, *Biomacromolecules* **2009**, *10*, 2694.
- [51] T. Gao, G. J. Gillispie, J. S. Copus, A. P. R. Kumar, Y.-J. Seol, A. Atala, J. J. Yoo, S. J. Lee, *Biofabrication* **2018**, *10*, 034106.
- [52] T. Iskratsch, H. Wolfenson, M. P. Sheetz, *Nat. Rev. Mol. Cell Biol.* **2014**, *15*, 825.
- [53] A. J. Engler, S. Sen, H. L. Sweeney, D. E. Discher, *Cell* **2006**, *126*, 677.
- [54] C. M. Lo, H. B. Wang, M. Dembo, Y. L. Wang, *Biophys. J.* **2000**, *79*, 144.
- [55] T. Yeung, P. C. Georges, L. A. Flanagan, B. Marg, M. Ortiz, M. Funaki, N. Zahir, W. Ming, V. Weaver, P. A. Janmey, *Cell Motil. Cytoskeleton* **2005**, *60*, 24.
- [56] E. Hadjipanayi, V. Mudera, R. A. Brown, *J. Tissue Eng. Regener. Med.* **2009**, *3*, 77.
- [57] K. C. Spencer, J. C. Sy, K. B. Ramadi, A. M. Graybiel, R. Langer, M. J. Cima, *Sci. Rep.* **2017**, *7*, 1952.
- [58] O. Chaudhuri, J. Cooper-White, P. A. Janmey, D. J. Mooney, V. B. Shenoy, *Nature* **2020**, *584*, 535.
- [59] O. Chaudhuri, L. Gu, D. Klumpers, M. Darnell, S. A. Bencherif, J. C. Weaver, N. Huebsch, H. Lee, E. Lippens, G. N. Duda, D. J. Mooney, *Nat. Mater.* **2016**, *15*, 326.
- [60] O. Chaudhuri, L. Gu, M. Darnell, D. Klumpers, S. A. Bencherif, J. C. Weaver, N. Huebsch, D. J. Mooney, *Nat. Commun.* **2015**, *6*, 6365.
- [61] D. B. Kolesky, K. A. Homan, M. A. Skylar-Scott, J. A. Lewis, *Proc. Natl. Acad. Sci. USA* **2016**, *113*, 3179.
- [62] W. Wu, A. Deconinck, J. A. Lewis, *Adv. Mater.* **2011**, *23*, H178.
- [63] T. Bhattacharjee, S. M. Zehnder, K. G. Rowe, S. Jain, R. M. Nixon, W. G. Sawyer, T. E. Angelini, *Sci. Adv.* **2015**, *1*, e1500655.
- [64] T. J. Hinton, Q. Jallerat, R. N. Palchesko, J. H. Park, M. S. Grodzicki, H. J. Shue, M. H. Ramadan, A. R. Hudson, A. W. Feinberg, *Sci. Adv.* **2015**, *1*, e1500758.
- [65] C. B. Highley, C. B. Rodell, J. A. Burdick, *Adv. Mater.* **2015**, *27*, 5075.
- [66] A. McCormack, C. B. Highley, N. R. Leslie, F. P. W. Melchels, *Trends Biotechnol.* **2020**, *38*, 584.
- [67] D. J. Shiawski, A. R. Hudson, J. W. Tashman, A. W. Feinberg, *APL Bioeng.* **2021**, *5*, 10904.
- [68] U. Hersel, C. Dahmen, H. Kessler, *Biomaterials* **2003**, *24*, 4385.
- [69] M. Barczyk, S. Carracedo, D. Gullberg, *Cell Tissue Res.* **2010**, *339*, 269.

- [70] E. Ruoslahti, M. D. Pierschbacher, *Science* **1987**, 238, 491.
- [71] H. G. Yi, Y. H. Jeong, Y. Kim, Y. J. Choi, H. E. Moon, S. H. Park, K. S. Kang, M. Bae, J. Jang, H. Youn, S. H. Paek, D. W. Cho, *Nat. Biomed. Eng.* **2019**, 3, 509.
- [72] J. Jang, T. G. Kim, B. S. Kim, S. W. Kim, S. M. Kwon, D. W. Cho, *Acta Biomater.* **2016**, 33, 88.
- [73] K. Jakab, C. Norotte, F. Marga, K. Murphy, G. Vunjak-Novakovic, G. Forgacs, *Biofabrication* **2010**, 2, 022001.
- [74] G. Gao, J. H. Lee, J. Jang, D. H. Lee, J. S. Kong, B. S. Kim, Y. J. Choi, W. B. Jang, Y. J. Hong, S. M. Kwon, D. W. Cho, *Adv. Funct. Mater.* **2017**, 27, 1700798.
- [75] M. Ali, P. R. Anil Kumar, J. J. Yoo, F. Zahran, A. Atala, S. J. Lee, *Adv. Healthcare Mater.* **2019**, 8, 1800992.
- [76] L. L. Wang, C. B. Highley, Y.-C. Yeh, J. H. Galarraga, S. Uman, J. A. Burdick, *J. Biomed. Mater. Res., Part A* **2018**, 106, 865.
- [77] J. Lee, A. R. Unnithan, C. H. Park, C. S. Kim, *Biomimetic Nanoengineered Materials for Advanced Drug Delivery*, Elsevier, Amsterdam **2019**, pp. 61–72.
- [78] M. Lee, K. Bae, C. Levinson, M. Zenobi-Wong, *Biofabrication* **2020**, 12, 25025.
- [79] F. L. C. Morgan, L. Moroni, M. B. Baker, *Adv. Healthcare Mater.* **2020**, 9, 1901798.
- [80] A. Lee, A. R. Hudson, D. J. Shiawski, J. W. Tashman, T. J. Hinton, S. Yerneni, J. M. Bliley, P. G. Campbell, A. W. Feinberg, *Science* **2019**, 365, 482.
- [81] S. M. Hull, C. D. Lindsay, L. G. Brunel, D. J. Shiawski, J. W. Tashman, J. G. Roth, D. Myung, A. W. Feinberg, S. C. Heilshorn, *Adv. Funct. Mater.* **2020**, 31, 2007983.
- [82] M. Hospodiu, M. Dey, D. Sosnoski, I. T. Ozbolat, *Biotechnol. Adv.* **2017**, 35, 217.
- [83] S. Khalil, W. Sun, *J. Biomech. Eng.* **2009**, 131, 111002.
- [84] J. Jia, D. J. Richards, S. Pollard, Y. Tan, J. Rodriguez, R. P. Visconti, T. C. Trusk, M. J. Yost, H. Yao, R. R. Markwald, Y. Mei, *Acta Biomater.* **2014**, 10, 4323.
- [85] C. D. Lindsay, J. G. Roth, B. L. LeSavage, S. C. Heilshorn, *Acta Biomater.* **2019**, 95, 225.
- [86] J. Hazur, R. Detsch, E. Karakaya, J. Kaschta, J. Teßmar, D. Schneidereit, O. Friedrich, D. W. Schubert, A. R. Boccaccini, *Biofabrication* **2020**, 12, 045004.
- [87] N. Cao, X. B. Chen, D. J. Schreyer, *ISRN Chem. Eng.* **2012**, 2012, 516461.
- [88] K. Dubbin, Y. Hori, K. K. Lewis, S. C. Heilshorn, *Adv. Healthcare Mater.* **2016**, 5, 2488.
- [89] W. Jia, P. S. Gungor-Ozkerim, Y. S. Zhang, K. Yue, K. Zhu, W. Liu, Q. Pi, B. Byambaa, M. R. Dokmeci, S. R. Shin, A. Khademhosseini, *Biomaterials* **2016**, 106, 58.
- [90] L. Ouyang, C. B. Highley, C. B. Rodell, W. Sun, J. A. Burdick, *ACS Biomater. Sci. Eng.* **2016**, 2, 1743.
- [91] R. F. Pereira, B. N. Lourenço, P. J. Bártoolo, P. L. Granja, *Adv. Healthcare Mater.* **2020**, 10, 2001176.
- [92] J. Van Hoorick, L. Tytgat, A. Dobos, H. Ottevaere, J. Van Erps, H. Thienpont, A. Ovsianikov, P. Dubrule, S. Van Vlierberghe, *Acta Biomater.* **2019**, 97, 46.
- [93] R. F. Pereira, P. J. Bártoolo, *J. Appl. Polym. Sci.* **2015**, 132, 42458.
- [94] J. Y. Shin, Y. H. Yeo, J. E. Jeong, S. A. Park, W. H. Park, *Carbohydr. Polym.* **2020**, 238, 116192.
- [95] M. Kesti, M. Müller, J. Becher, M. Schnabelrauch, M. D'Este, D. Eglin, M. Zenobi-Wong, *Acta Biomater.* **2015**, 11, 162.
- [96] L. Ouyang, J. P. K. Armstrong, Y. Lin, J. P. Wojciechowski, C. Lee-Reeves, D. Hachim, K. Zhou, J. A. Burdick, M. M. Stevens, *Sci. Adv.* **2020**, 6, eabc5529.
- [97] N. Noor, A. Shapira, R. Edri, I. Gal, L. Wertheim, T. Dvir, *Adv. Sci.* **2019**, 6, 1900344.
- [98] A. L. Rutz, P. L. Lewis, R. N. Shah, *MRS Bull.* **2017**, 42, 563.
- [99] N. E. Fedorovich, M. H. Oudshoorn, D. van Geemen, W. E. Hennink, J. Alblas, W. J. A. Dhert, *Biomaterials* **2009**, 30, 344.
- [100] L. Ouyang, C. B. Highley, W. Sun, J. A. Burdick, *Adv. Mater.* **2017**, 29, 1604983.
- [101] B. G. Soliman, G. C. J. Lindberg, T. Jungst, G. J. Hooper, J. Groll, T. B. F. Woodfield, K. S. Lim, *Adv. Healthcare Mater.* **2020**, 9, 1901544.
- [102] K. S. Lim, B. S. Schon, N. V. Mekhileri, G. C. J. Brown, C. M. Chia, S. Prabakar, G. J. Hooper, T. B. F. Woodfield, *ACS Biomater. Sci. Eng.* **2016**, 2, 1752.
- [103] A. L. Rutz, K. E. Hyland, A. E. Jakus, W. R. Burghardt, R. N. Shah, *Adv. Mater.* **2015**, 27, 1607.
- [104] A. L. Rutz, E. S. Gargus, K. E. Hyland, P. L. Lewis, A. Setty, W. R. Burghardt, R. N. Shah, *Acta Biomater.* **2019**, 99, 121.
- [105] A. Basu, A. Saha, C. Goodman, R. T. Shafranek, A. Nelson, *ACS Appl. Mater. Interfaces* **2017**, 9, 40898.
- [106] K. H. Song, C. B. Highley, A. Rouff, J. A. Burdick, *Adv. Funct. Mater.* **2018**, 28, 1801331.
- [107] O. Jeon, Y. B. Lee, T. J. Hinton, A. W. Feinberg, E. Alsberg, *Mater. Today Chem.* **2019**, 12, 61.
- [108] K. Zhu, N. Chen, X. Liu, X. Mu, W. Zhang, C. Wang, Y. S. Zhang, *Macromol. Biosci.* **2018**, 18, 1800127.
- [109] W. Lim, G. J. Kim, H. W. Kim, J. Lee, X. Zhang, M. G. Kang, J. W. Seo, J. M. Cha, H. J. Park, M. Y. Lee, S. R. Shin, S. Y. Shin, H. Bae, *Polymers* **2020**, 12, 2377.
- [110] T. Hu, X. Cui, M. Zhu, M. Wu, Y. Tian, B. Yao, W. Song, Z. Niu, S. Huang, X. Fu, *Bioact. Mater.* **2020**, 5, 808.
- [111] A. Skardal, M. Devarasetty, H. W. Kang, I. Mead, C. Bishop, T. Shupe, S. J. Lee, J. Jackson, J. Yoo, S. Soker, A. Atala, *Acta Biomater.* **2015**, 25, 24.
- [112] D. Petta, A. R. Armiento, D. Grijpma, M. Alini, D. Eglin, M. D'Este, *Biofabrication* **2018**, 10, 44104.
- [113] H. D. Lu, D. E. Soranno, C. B. Rodell, I. L. Kim, J. A. Burdick, *Adv. Healthcare Mater.* **2013**, 2, 1028.
- [114] H. Wang, D. Zhu, A. Paul, L. Cai, A. Enejder, F. Yang, S. C. Heilshorn, *Adv. Funct. Mater.* **2017**, 27, 1605609.
- [115] R. F. Pereira, A. Sousa, C. C. Barrias, P. J. Bártoolo, P. L. Granja, *Mater. Horiz.* **2018**, 5, 1100.
- [116] M. J. Glassman, J. Chan, B. D. Olsen, *Adv. Funct. Mater.* **2013**, 23, 1182.
- [117] L. Shi, F. Wang, W. Zhu, Z. Xu, S. Fuchs, J. Hilborn, L. Zhu, Q. Ma, Y. Wang, X. Weng, D. A. Ossipov, *Adv. Funct. Mater.* **2017**, 27, 1700591.
- [118] A. N. Leberfinger, S. Dinda, Y. Wu, S. V. Koduru, V. Ozbolat, D. J. Ravnic, I. T. Ozbolat, *Acta Biomater.* **2019**, 95, 32.
- [119] R. L. Mauck, C. C. B. Wang, E. S. Oswald, G. A. Ateshian, C. T. Hung, *Osteoarthritis Cartilage* **2003**, 11, 879.
- [120] S. C. N. Chang, J. A. Rowley, G. Tobias, N. G. Genes, A. K. Roy, D. J. Mooney, C. A. Vacanti, L. J. Bonassar, *J. Biomed. Mater. Res.* **2001**, 55, 503.
- [121] M. Ahearne, *Interface Focus* **2014**, 4, 20130038.
- [122] T. Billiet, E. Gevaert, T. De Schryver, M. Cornelissen, P. Dubrule, *Biomaterials* **2014**, 35, 49.
- [123] A. Skardal, J. Zhang, G. D. Prestwich, *Biomaterials* **2010**, 31, 6173.
- [124] K. Hölzl, S. Lin, L. Tytgat, S. Van Vlierberghe, L. Gu, A. Ovsianikov, *Biofabrication* **2016**, 8, 032002.
- [125] M. A. Skylar-Scott, S. G. M. Uzel, L. L. Nam, J. H. Ahrens, R. L. Truby, S. Damaraju, J. A. Lewis, *Sci. Adv.* **2019**, 5, eaaw2459.
- [126] H. Ding, F. Tourlomousis, R. C. Chang, *Biomed. Phys. Eng. Express* **2017**, 3, 035016.
- [127] V. Mironov, R. P. Visconti, V. Kasyanov, G. Forgacs, C. J. Drake, R. R. Markwald, *Biomaterials* **2009**, 30, 2164.
- [128] A. M. Blakely, K. L. Manning, A. Tripathi, J. R. Morgan, *Tissue Eng., Part C* **2015**, 21, 737.

- [129] A. Cristea, A. Neagu, *Comput. Biol. Med.* **2016**, *70*, 80.
- [130] H. Bae, A. F. Ahari, H. Shin, J. W. Nichol, C. B. Hutson, M. Masaeli, S. H. Kim, H. Aubin, S. Yamanlar, A. Khademhosseini, *Soft Matter* **2011**, *7*, 1903.
- [131] C. Cha, S. R. Shin, X. Gao, N. Annabi, M. R. Dokmeci, X. Tang, A. Khademhosseini, *Small* **2014**, *10*, 514.
- [132] B. H. Lee, B. Li, S. A. Guelcher, *Acta Biomater.* **2012**, *8*, 1693.
- [133] B. Wehrle-Haller, *Curr. Opin. Cell Biol.* **2012**, *24*, 569.
- [134] N. Q. Balaban, U. S. Schwarz, D. Riveline, P. Goichberg, G. Tzur, I. Sabanay, D. Mahalu, S. Safran, A. Bershadsky, L. Addadi, B. Geiger, *Nat. Cell Biol.* **2001**, *3*, 466.
- [135] C. D. Morley, S. T. Ellison, T. Bhattacharjee, C. S. O'Bryan, Y. Zhang, K. F. Smith, C. P. Kabb, M. Sebastian, G. L. Moore, K. D. Schulze, S. Niemi, W. G. Sawyer, D. D. Tran, D. A. Mitchell, B. S. Sumerlin, C. T. Flores, T. E. Angelini, *Nat. Commun.* **2019**, *10*, 3029.
- [136] K. Kurabayashi-Shigetomi, H. Onoe, S. Takeuchi, *PLoS One* **2012**, *7*, e51085.
- [137] J. Y. Schell, B. T. Wilks, M. Patel, C. Franck, V. Chalivendra, X. Cao, V. B. Shenoy, J. R. Morgan, *Biomaterials* **2016**, *77*, 120.
- [138] D.-W. Cho, *Biofabrication and 3D Tissue Modeling*, Royal Society of Chemistry, London **2019**.
- [139] T. Ikegami, Y. Maebara, *Nat. Rev. Gastroenterol. Hepatol.* **2013**, *10*, 697.
- [140] A. Metters, J. Hubbell, *Biomacromolecules* **2005**, *6*, 290.
- [141] A. M. Kloxin, A. M. Kasko, C. N. Salinas, K. S. Anseth, *Science* **2009**, *324*, 59.
- [142] A. M. Kloxin, M. W. Tibbitt, A. M. Kasko, J. A. Fairbairn, K. S. Anseth, *Adv. Mater.* **2010**, *22*, 61.
- [143] A. Sydney Gladman, E. A. Matsumoto, R. G. Nuzzo, L. Mahadevan, J. A. Lewis, *Nat. Mater.* **2016**, *15*, 413.
- [144] D. N. Heo, M. A. Alioglu, Y. Wu, V. Ozbolat, B. Ayan, M. Dey, Y. Kang, I. T. Ozbolat, *ACS Appl. Mater. Interfaces* **2020**, *12*, 20295.
- [145] J. H. Shim, J. S. Lee, J. Y. Kim, D. W. Cho, *J. Micromech. Microeng.* **2012**, *22*, 085014.
- [146] T. Möller, M. Amoroso, D. Hägg, C. Brantsing, N. Rotter, P. Apelgren, A. Lindahl, L. Kölby, P. Gatenholm, *Plast. Reconstr. Surg. Global Open* **2017**, *5*, e1227.
- [147] J. Lou, F. Liu, C. D. Lindsay, O. Chaudhuri, S. C. Heilshorn, Y. Xia, *Adv. Mater.* **2018**, *30*, 1705215.
- [148] M. Barbosa, M. C. L. Martins, P. Gomes, *Gels* **2015**, *1*, 194.
- [149] K. A. Kilian, M. Mrksich, *Angew. Chem.* **2012**, *2*, 4891.
- [150] X. Tong, F. Yang, *Adv. Mater.* **2016**, *28*, 7257.
- [151] N. Gjorevski, N. Sachs, A. Manfrin, S. Giger, M. E. Bragina, P. Ordóñez-Morán, H. Clevers, M. P. Lutolf, *Nature* **2016**, *539*, 560.
- [152] R. Cruz-acuña, M. Quirós, A. E. Farkas, P. H. Dedhia, S. Huang, D. Siuda, V. García-hernández, A. J. Miller, J. R. Spence, A. Nusrat, A. J. García, *Nat. Cell Biol.* **2017**, *19*, 1326.
- [153] J. Lam, N. F. Truong, T. Segura, *Acta Biomater.* **2014**, *10*, 1571.
- [154] K. A. Mosiewicz, L. Kolb, A. J. Van Der Vlies, M. M. Martino, P. S. Lienemann, J. A. Hubbell, M. Ehrbar, M. P. Lutolf, *Nat. Mater.* **2013**, *12*, 1072.
- [155] F. E. Freeman, P. Pitacco, L. H. A. van Dommelen, J. Nulty, D. C. Browe, J. Y. Shin, E. Alsberg, D. J. Kelly, *Sci. Adv.* **2020**, *6*, eabb5093.
- [156] J. Zhu, A. Mogilner, *Interface Focus* **2016**, *6*, 20160040.
- [157] J. K. Mouw, G. Ou, V. M. Weaver, *Nat. Rev. Mol. Cell Biol.* **2014**, *15*, 771.
- [158] W. Y. Wang, A. T. Pearson, M. L. Kutys, C. K. Choi, M. A. Wozniak, B. M. Baker, C. S. Chen, *APL Bioeng.* **2018**, *2*, 046107.
- [159] E. D. F. Ker, A. S. Nain, L. E. Weiss, J. Wang, J. Suhan, C. H. Amon, P. G. Campbell, *Biomaterials* **2011**, *32*, 8097.
- [160] L. Riley, L. Schirmer, T. Segura, *Curr. Opin. Biotechnol.* **2019**, *60*, 1.
- [161] C. B. Highley, K. H. Song, A. C. Daly, J. A. Burdick, *Adv. Sci.* **2019**, *6*, 1801076.
- [162] A. J. Seymour, S. Shin, S. C. Heilshorn, *Adv. Healthcare Mater.* **2021**, *10*, 2100644.
- [163] V. X. Truong, K. M. Tsang, J. S. Forsythe, *Biomacromolecules* **2017**, *18*, 757.
- [164] H. Holback, Y. Yeo, K. Park, *Hydrogel Swelling Behavior and Its Biomedical Applications*, Woodhead Publishing Limited, Cambridge **2011**.
- [165] M. Nikkhah, J. S. Strobl, M. Agah, *Biomed. Microdevices* **2009**, *11*, 429.
- [166] M. Jamal, S. S. Kadam, R. Xiao, F. Jivan, T. M. Onn, R. Fernandes, T. D. Nguyen, D. H. Gracias, *Adv. Healthcare Mater.* **2013**, *2*, 1142.
- [167] H. R. Kwag, J. V. Serbo, P. Korangath, S. Sukumar, L. H. Romer, D. H. Gracias, *Tissue Eng., Part C* **2016**, *22*, 398.
- [168] C. Correia, A. L. Pereira, A. R. C. Duarte, A. M. Frias, A. J. Pedro, J. T. Oliveira, R. A. Sousa, R. L. Reis, *Tissue Eng., Part A* **2012**, *18*, 1979.
- [169] E. Mooney, J. N. Mackle, D. J. P. Blond, E. O'Cearbhail, G. Shaw, W. J. Blau, F. P. Barry, V. Barron, J. M. Murphy, *Biomaterials* **2012**, *33*, 6132.
- [170] C. W. Hsiao, M. Y. Bai, Y. Chang, M. F. Chung, T. Y. Lee, C. T. Wu, B. Maiti, Z. X. Liao, R. K. Li, H. W. Sung, *Biomaterials* **2013**, *34*, 1063.



Sarah M. Hull is pursuing her Ph.D. at Stanford University in the Department of Chemical Engineering. She obtained her B.S. degree in chemical engineering from the University of California, Berkeley in 2016. Her research interests include 3D bioprinting, dynamic hydrogels, mechanobiology, and regenerative therapies for the eye. Her current work focuses on new crosslinking strategies for bioink design in order to create inks that are biochemically and mechanically customizable for different cell types.



Lucia G. Brunel is a doctoral candidate in chemical engineering at Stanford University. She previously obtained her B.S. and M.S. degrees in chemical engineering from Northwestern University (Goldwater Scholar) in 2018 and her M.Phil. degree in materials science from the University of Cambridge (Marshall Scholar) in 2019. Her research interests are in polymeric biomaterials as scaffolds for in vitro tissue models. Her current work focuses on the design of hydrogels with hierarchical features to guide the phenotype of encapsulated cells, and on crosslinking chemistries that enable their use as bioinks for 3D bioprinting.



Sarah C. Heilshorn is a professor and associate chair in the Materials Science and Engineering Department at Stanford University, where she also serves as the director of the Geballe Laboratory for Advanced Materials. Her research team integrates concepts from materials science and protein engineering to design bioinspired materials for regenerative medicine, organoid culture, and bioprinting. She is a fervent supporter of diversifying the scientific research community. She is a fellow of the American Institute for Medical and Biological Engineering and the Royal Society of Chemistry, and serves on the Board of Directors for the Materials Research Society and the International Society for Biofabrication.